UNIVERSITY OF LEEDS

This is a repository copy of *Rapid synthesis and electrical transition in p-type delafossite $CuAlO_2$*.

White Rose Research Online URL for this paper:
http://eprints.whiterose.ac.uk/99444/

Version: Accepted Version

Article:
Mudenda, S, Kale, GM and Hara, YRS (2014) Rapid synthesis and electrical transition in p-type delafossite $CuAlO_2$. Journal of Materials Chemistry C, 2 (43). pp. 9233-9239. ISSN 2050-7526

https://doi.org/10.1039/c4tc01349b

Reuse
Unless indicated otherwise, fulltext items are protected by copyright with all rights reserved. The copyright exception in section 29 of the Copyright, Designs and Patents Act 1988 allows the making of a single copy solely for the purpose of non-commercial research or private study within the limits of fair dealing. The publisher or other rights-holder may allow further reproduction and re-use of this version - refer to the White Rose Research Online record for this item. Where records identify the publisher as the copyright holder, users can verify any specific terms of use on the publisher's website.

Takedown
If you consider content in White Rose Research Online to be in breach of UK law, please notify us by emailing eprints@whiterose.ac.uk including the URL of the record and the reason for the withdrawal request.

eprints@whiterose.ac.uk
https://eprints.whiterose.ac.uk/

CREATED USING THE RSC LaTeX PCCP ARTICLE TEMPLATE – SEE www.rsc.org/electronicfiles FOR DETAILS

Rapid synthesis and electrical transition in *p*-type delafossite $CuAlO_2$

Steven MUDENDA, Girish M. KALE* and Yotamu R.S HARA

Received Xth XXXXXXXXXX 20XX, Accepted Xth XXXXXXXXX 20XX
First published on the web Xth XXXXXXXXXX 200X
DOI: 10.1039/b000000x

Highly polycrystalline and pure delafossite phase $CuAlO_2$ powder has been synthesised within a short annealing period, shorter than most conventional processes. This is an improvement over the conventional synthesis procedures. Conventional synthesis procedure has seen $CuAlO_2$ only formed at high annealing temperatures $\geq$ 1100 °C over long annealing time, some as long as 96 hours. In the current process, a pure phase devoid of impurities has been obtained at reduced calcination time of 1.5 hours in an argon atmosphere at a temperature of 1150 °C. This was confirmed by XRD and SEM/EDX. High temperature DC/AC electrical measurements show a change in conduction mechanism from mixed conductivity (ionic + *p*-type) in the temperature range of $375 \geq T \geq 25$ °C to intrinsic type behavior above 375 °C. The activation energies for these two regimes are 0.27 eV and 0.08 eV respectively. This change from mixed to DC conductivity is confirmed by spectral analysis too. Spectral analysis using the power law also revealed that conduction is of long range hopping. Use of platinum as a contact electrode at elevated temperatures has a detrimental effect on the electrical properties since it encourages the formation of $CuAl_2O_4$ at the interface due to the formation of more stable Cu−Pt alloy by virtue of the chemical reaction $Pt + 2CuAlO_2 \rightarrow CuAl_2O_4 + \underline{Pt}_{Cu}$.

1 Introduction

$CuAlO_2$ (CAO) is a delafossite *p*-type semiconductor with a band gap of ≥ 3.0 eV[1,2]. The visible transmittance of the CAO can be as high as 80%, suggesting that CAO can be considered as an ideal candidate for p-type transparent conductive oxides (TCOs)[3].

TCOs find applications in a wide range of optoelectronics devices such as solar cells, flat panel displays and touch panel controls as transparent electrodes. Most of the transparent films are made up of n-type semiconductors from oxides and their doped versions of SnO_2 , In_2O_3, ZnO[4,5]. These are readily available. However in the formulation of p-n junctions meant for transparent elements such as transistors and diodes, transparent p-type semiconductors are required. Their development has been a challenge as observed by Scanlon and Smith[6]. It was not until 1997 when Kawazoe and co-workers first reported a simulteneous p-type conductivity and optical transparency of the $CuAlO_2$ thin films[2] that spurred extensive research for these type of materials and led to a discovery of many other delafossite-type compounds such as $CuMO_2$: (M= B, Cr, Sc, Y, Eu, Ga)[7] and $SrCu_2O_2$[8].

The origin of *p*-type conductivity of undoped $CuAlO_2$ is still controversial but it is generally accepted that it is mainly due to Cu-site holes[9], small polaron transport[10] and variable range hopping (VRH)[10,11]. The conductivity is highly anisotropic due to its structure[12]. CAO thin films are generally prepared by pulsed laser deposition (PLD)[2], spray pyrolysis[13], chemical vapour deposition[14], sputtering[15–18]. TCO thin films for optoelectronics devices such as transparent solar cells and flat panel displays are commercially deposited using RF sputtering because of its capability of producing high purity thin films at lower temperatures. Therefore, to improve the properties of the TCO targets and the sputtered thin films, high quality phase pure powders of CAO are required for the sputter targets.

A number of methods have been employed for the synthesis of bulk CAO, such as wet chemical synthesis (sol-gel, hydrothermal)[3,5,19–21], slow cooling reactions from melts of $CuAl_2O_4 + CuO$[22] and the conventional method involving a prolonged solid state reaction of Cu_2O and Al_2O_3[2,15,23,24]. Other solid state reactions involving boehmite (AlOOH) and Cu_2O have also been reported recently[25,26]. The synthesis temperatures involved here are always in the excess of 1100 °C and for prolonged reaction times, ranging from 3 to 96 hours as shown in Table 1. Despite all this, obtaining single phases and well crystallined material has been a problem as observed from their XRD patterns. Recently, Jarman *et al.*[27] synthesized CAO using the Pechini method and obtained a pure phase at the reaction time of 3 h. Despite the success, the number of stages and reagents involved for the preparation for the CAO still make the conventional process economical and less involving. Amrute *et al.*[24] also synthesised CAO using solid state reaction, one in air and the other one in nitrogen atmosphere. After 30 h of reaction at 1100 °C, CAO reacted in air was 100 % pure while nitrogen environment obtained only 70 % pure CAO. In our investigation, it has been shown that argon environment and quenching reacted products under graphite effectively produces a 100 % pure CAO in just 1.5 h.

* *Tel: 0044-113-3432805 ; E-mail: g.m.kale@leeds.ac.uk*
Institute For Materials Research, University of Leeds, LS2 9JT, UK

The energy saved is many magnitudes better than the processes with reaction temperatures and durations in Table 1. Table 1 shows the general calcination temperatures and reaction time for the synthesis of CAO powders by various researchers.

Table 1 Calcination temperatures and durations for the synthesis of CAO. **WC: Wet Chemical, SS: Solid State.**

Method	T (°C)	Dur. (h)	Environ.	Refs
SS	1100	10/2.	N_2/air	[26]
SS	1150	2 resp.	Ar	[25]
SS	1100	>30/30	N_2/ air	[24]
WC	1100/800	24/48	air/N_2	[21]
WC	320/400	12/4	-	[20]
SS	1050 /1200	96/5 .	air	[28]
WC	1100	11	air	[3]
WC	1100	3	air	[27]
SS	1102	24	-	[15]
WC/SS	1100	6/15	-	[29]
SS	1100	24/36	air	[23]
SS	1100	10	-	[30]
SS	1100	20	air	[31]
SS	1200	12	air	[17]
WC	1200	4	air	[19]
SS	1100	72	vacuum	[32]

In this paper we report a procedure where CAO was obtained at a much lower temperature and in short reaction time using the conventional method of reacting Cu_2O and Al_2O_3. A phase pure powder was obtained as seen from the XRD pattern. The process involved milling, powder pelletizing, isothermal firing under argon and quenching.

2 Experimental

2.1 Thermodynamics Considerations

From the Al_2O_3 - $\frac{1}{2}Cu_2O/CuO$ phase diagram by Jacob and Alcock [32], the upper temperature stability limit of the $CuAlO_2$ phase is 1160 °C at $P_{O_2} = 0.21$ atm. This means that the reactions (formation of CAO) can only be carried out at temperatures below 1160 °C. Considering the fact that the melting points of Cu_2O and Al_2O_3 are 1232 °C and 2072 °C respectively and, the absence of the eutectic melts below 1160 °C in the Al_2O_3- Cu_2O system, the formation of the $CuAlO_2$ phase is a solid state mechanism. Since solid state reactions occur via diffusion of the cations, a higher temperature is required to enhance the diffusion since the diffusion of these species is very slow at low temperature. The calcination temperature of 1150 °C was therefore ideal and gave the shortest reaction time.

2.2 Methodology

Appropriate amounts of precursor oxides, Cu_2O (95% purity, Scientific Laboratory Supplies) and $\gamma-Al_2O_3$ (99.7% purity, SIGMA-Aldrich), were weighed and mixed in a plastic milling jar. Zirconia balls and isopropranol were used as milling media. The precursor powders were then milled overnight. After milling, the slurry was dried into homogeneously mixed powder. The powder was pressed into a cylindrical pellets at loads of 1,4 and 8 tonnes using a 13 mm diameter uniaxial steel die. This was meant to bring the reacting particles in intimate contact with each other for easy reaction. The samples in the form of loose powder and pellets were isothermally fired at 1150 °C for *ca* 1.5 h under flowing argon environment to prevent oxidation of the Cu_2O. Isothermal firing is when the sample is placed in the already hot furnace at that target temperature and then removed from the furnace at the same temperature. After 1.5 h of firing, the samples were removed from the furnace and cooled under the cover of a graphite crucible so as to prevent any possible oxidation of $Cu^+ \rightarrow Cu^{2+}$ in the reacted products.

For electrical characterisations, a pellet uniaxially pressed under a load of 5 tonnes and sintered in air at 1150 °C for 6 h was used. Platinum ink was painted on the parallel sides of the pellet as electrode contacts and cured at 800 °C for 30 minutes. The sample was spring loaded in a quartz assembly placed inside a Faraday cage within a horizontal tube furnace during the AC/DC electrical measurements. The DC conductivity measurements were conducted using the Hewlett Packard 34420A NanoVolt/Micro Ohm meter and AC conductivity measurements using the Solartron Instrument 1260. For phase analysis of the samples by XRD, the samples were ground into fine powder and analysed using the P'Analytical X'Pert MPD (using Cu K_α radiation) in a spinning mode. Morphological features and EDX (for chemical composition) were obtained using the LEO Gemini 1530 field emission scanning electron microscope.

This journal is © The Royal Society of Chemistry [year]

3 Results and Discussion

3.1 *XRD*

Fig. 1 shows XRD patterns of the CAO powder and pellets annealed at 1150 °C for 1.5 h under argon atmosphere. To study the effect of pelletising, unpelletised samples were also characterised as a control. It can clearly be seen from the XRD patterns in Fig. 1, especially of the pellets, that a pure phase devoid of any detectable impurity phase or unreacted precursors was formed. This exactly matches with the standard, ICDD 04-010-0381 pattern. However, for the unpelletised sample, very low intensity XRD peaks for CuO at $2\theta = 36°, 38°$ can be seen. The presence of CuO clearly indicates that the unpelletised sample did not fully react during the 1.5 h isothermal heating. As a result, the unreacted Cu_2O might have oxidised when removing the sample from the furnace after isothermal heat treatment. The CAO peaks are also very intense showing a high degree of crystallinity.

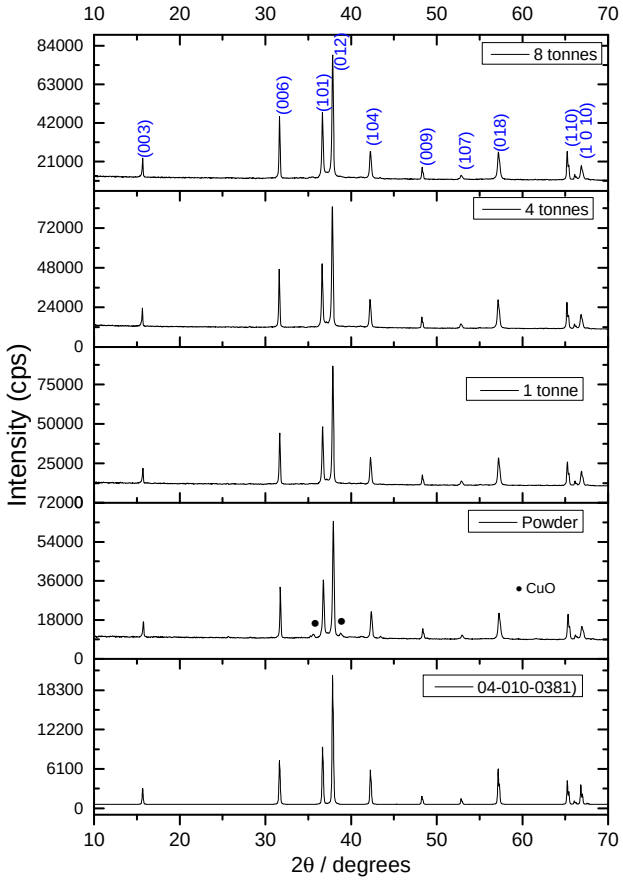

Fig. 1 XRD reflection data on the powder, and pellets pressed at different loads. At the bottom the standard (ICDD 04-010-0381) is shown as well.

It was also observed that the pelletising load had no observable effect on the kinetics of the reaction, since all pelletised samples gave pure $CuAlO_2$. From this observation, it can therefore be concluded that it is important to pelletise the samples regardless of the amount of load. Results from the same work, not included here showed that increasing the reaction time above 1.5 h, all samples (powders and pellets) produced a pure $CuAlO_2$ phase. Hence it seems that 1.5 h duration is the lower limit for obtaining a pure phase in pellets at 1150 °C.

The success of the procedure that has ensured a phase pure $CuAlO_2$ within 1.5 h of reaction may be because of (a) the inert environment which inhibits the oxidation of $Cu^+ \rightarrow Cu^{2+}$. This is because the oxide of Cu(I) is more reactive than the oxide of Cu(II) in ambient atmosphere at elevated temperatures[20,24,26]. Passing argon having low P_{O_2} helps preserve the reactive precursor for subsequent reaction. (b) pelletising brings reactive species in intimate contact for easy reaction. In addition, pelletizing guarantees that any trace of oxygen in the reaction furnace does not have access to the bulk of the material except for the surface of the pellet. (c) isothermal firing ensures that the intended reaction only takes place at a particular target temperature, instead of many side reactions which may inhibit or retard the intended formation of CAO due to the formation of CuO which is less reactive.

Furthermore, CuO and Al_2O_3 can react to form $CuAl_2O_4$ spinel as impurity in the CAO which can be detrimental for the optical and electrical properties of CAO[33]. (d) Quenching the sample under a graphite crucible. Quenching preserves the CAO phase by preventing the slow formation of $CuAl_2O_4$. This process is oxygen dependent, therefore quenching under the graphite crucible prevents CAO oxidation because graphite acts as an oxygen scavenger. Therefore, to obtain a pure and high quality CAO powder suitable for target in PLD applications, powder prepared by conventional method above and annealed at 1150 for 1.5 h would yield the much desired quality of CAO.

3.2 *SEM/EDX*

Fig. 2 shows an SEM image and results of EDX scan of the CAO powder annealed at 1150 °C. The top figure indicates that elongated grains are formed during calcination. The crystal growth seems to be more pronounced in one preferred direction. However, the grains are randomly oriented. This has negative effects on the electrical conductivity due to the anisotropic behaviour of the CAO[12,33]. The microstructure show that powder looks sintered at this temperature.

To confirm chemical composition, EDX measurements were performed over the sintered grain. The bottom image shows the scan area.

On the right side is the table of elemental composition. From the table, the ratio, Cu/Al = $\frac{24.14}{22.15} = 1.08$, suggesting that $CuAlO_2$ may be slightly non-stoichiometric having excess of Cu^+.

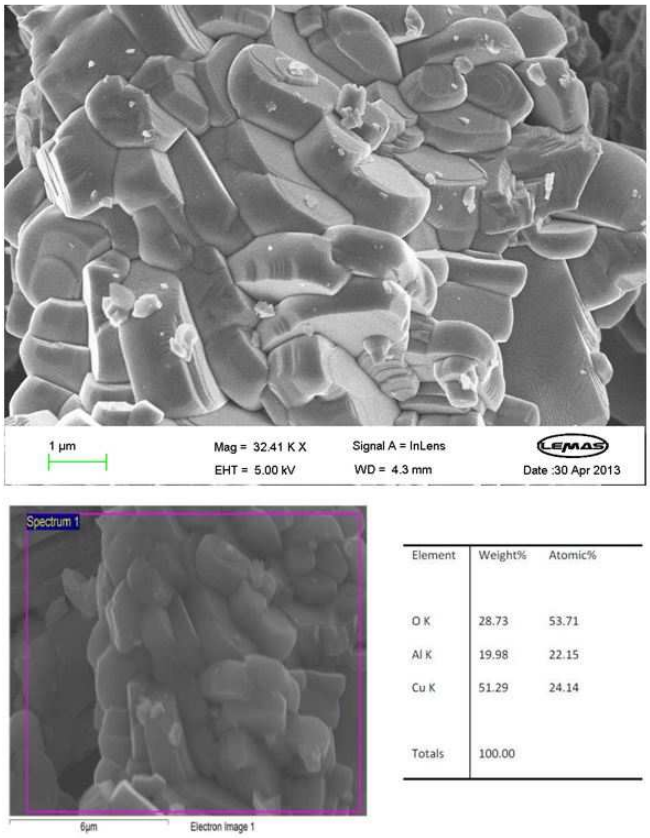

Fig. 2 EDX/SEM measurements on sintered CAO. The bottom image is the EDX.

3.3 *DC/AC Conductivity and Spectral Analysis*

3.3.1 Impedance Analysis. The temperature dependence of conductivity of CAO has been studied before but mostly below the room temperature (RT) by previous researchers Kawazoe *et al.*[2], Deng *et al.*[3], Lee. *et al.*[12]. These measurements were on thin films and employing DC measurements technique. Less work has been done on high temperature measurements, although some researchers[15,31,34] attempted to measure in the temperature range (in °C) of $302 \geq T \geq RT$. These were thin films too and used DC measurements. Prakash[31] used bulk samples and studied AC conductivity from 60 to 200 °C. In this study, high temperature DC and AC measurements were done over a temperature range of $711 \geq T \geq RT$ °C.

Fig. 3 shows the Nyquist plots from the AC measurements of the sample. As can clearly be seen from the semi-circular Cole-Cole plots, the material conducts ions too. The conduction is a polaronic thermally activated process. This can be seen from the semi circles' diameters decreasing with temperature. The conductivity continues to increase with temperature until a breakdown in ionic conductivity occurs at a temperature of 375 °C. At temperatures higher than 375 °C, no ionic conductivity is observed except for the inductive effects. This can be clearly seen in the inset of Fig. 3.

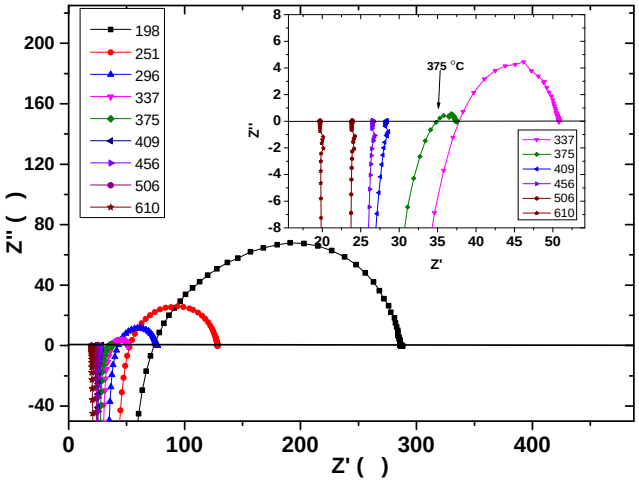

Fig. 3 AC Impedance measurements of CAO. The inset shows the temperatures at which there is a breakdown of ionic conductivity. After 375 °C ionic conductivity diminishes.

Temperature dependence of conductivity is represented by the Arrhenius relation in eqn(1);

$$\sigma = \sigma_0 \exp\left(-\frac{E_a}{kT}\right). \quad (1)$$

where; σ_0 is a pre-exponential factor which is a function of charge carrier concentration and material structural parameters, k is the Boltzmann constant and E_a is the activation energy of conduction.

A comparison of *p*-type (hole) conductivity (from DC measurements) and ionic conductivity (from AC impedance measurements) is shown in the Arrhenius plot in Fig. 4. The plot conforms to a polaronic thermally activated process. As can be seen from these two measurements, it is clear that the material is a mixed conductor (holes and ions) since both hole and ionic phenomena could be measured through DC and AC measurements respectively over a selected range of temperatures.

The plot attributed to the hole conductivity in the Arrhenius plot shows that DC conduction was reproducible as can be seen from the Fig. 4.

This journal is © The Royal Society of Chemistry [year]

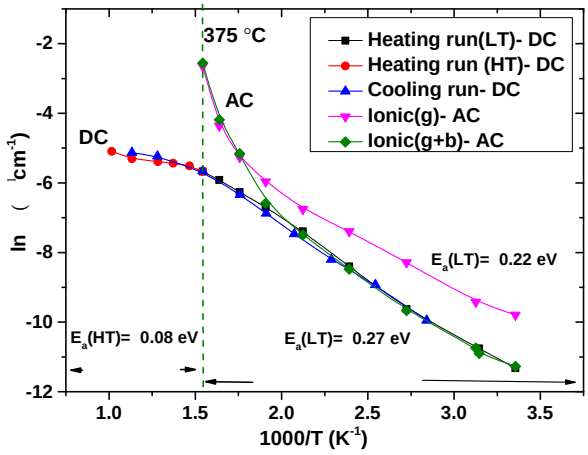

Fig. 4 Arrhenius for DC and AC Conductivities. Ionic(g) and ionic(g+b) are contributions from grains and grain+grain boundary respectively.

It can also be seen that conductivity exhibits two segments, high temperature (HT) and low temperature (LT). The slopes of the two segments yield the value of activation energy (E_a), which corresponds to the minimum energy required to transfer carriers from acceptor level to the valence band. The LT activation energy for DC conduction and AC grain conduction were $E_a(LT) = 0.27$ eV and $E_a(LT) = 0.22$ eV respectively. The values obtained in this study are in excellent agreement with each other and are within the range of activation energies reported in literature for both bulk and thin films in the temperature regimes of $T \geq RT$. Table 2 shows the activation energy as obtained by various research workers in comparison with the data obtained in this study.

In the present work, it has been shown for the first time that there is a HT regime which begins at 375 °C with an activation energy of $E_a(HT) = 0.08$ eV. This corresponds to the regime where hole conductivity completely dominates and the ionic conductivity ceases to exist. This is evident in the inset of Fig. 3. This result suggests a change in conduction mechanism from mixed conductivity (ionic + p-type) in the temperature range of $375 \geq T \geq 25$ °C to intrinsic type behavior above 375 °C. This is because at high temperatures carriers from acceptors become insignficant compared to the thermally generated carriers because of the complete ionization that takes place[37,38]. This behavior is a hallmark of most semiconductors. The transition temperature T_{trans} is related by

$$T_{trans} = E_g / k_B (N_C(T_{trans}) N_V(T_{trans})). \quad (2)$$

where $N_C(T_{trans})$ and $N_V(T_{trans})$ are the effective number of states in the conduction and valence band respectively, at a temperature close to the T_{trans}. The transition temperatures of different ternary adamantine semiconductors similar to delafossites are reported elsewhere[37] and this paper reports for the first time the T_{trans} for the delafossite CAO, being $T_{trans} \simeq 375$ °C.

The resistivity values obtained in this study are higher than those reported in literature probably because of two possible reasons: Firstly, the electrical conductivity in CAO appears to be anisotropic, $\sigma_{ab} = 25\sigma_c$ [12], where σ_{ab} is the conductivity in the a-b plane and σ_c the conductivity in the c-axis, whereas the random arrangement of grains in the bulk sample of the CAO as shown in the SEM images in Figure 2 may have played a part in giving rise to a lower conductivity of samples investigated in this study.

Secondly, the presence of an orange brown phase later identified as $CuAl_2O_4$ under the Pt electrical contact coating may have perhaps hindered charge transport. This was also observed by Lee. *et al.* [12]. After sample retrieval, it was also observed that part of the Pt coating on the sample surface of the pellet had delaminated as a result of the formation of $CuAl_2O_4$ phase at the interface between Pt and $CuAlO_2$, however, on the exposed circumference of the pellet that was uncoated, no signature of $CuAl_2O_4$ was seen. We believe this is due to the catalytic behaviour of Pt which promotes the formation of $CuAl_2O_4$ at the interface by virtue of the reaction : $Pt + 2CuAlO_2 \rightarrow CuAl_2O_4 + \underline{Pt}_{Cu}$. Under normal circumstances, the formation of $CuAl_2O_4$ from CAO according to $4\,CuAlO_2 + O_2 \rightarrow 2\,CuAl_2O_4 + 2\,CuO$ reaction which is P_{O_2} dependent is very slow especially at lower temperatures, below 1003 °C at 0.21 atm[39] also evident from our preliminary results. This implies that it is important to carefully select the contact electrode metal however noble that may be when it is to be placed in contact with another material containing copper. Further investigation on this topic will be reported in a separate communication in the near future.

3.3.2 Conductivity Spectral Analysis. Measurement of AC conductivity ($\sigma(\omega) = \sigma'(\omega) - j\sigma''(\omega)$) generally shows a frequency dispersion where, the real part of AC conductivity $\sigma'(\omega)$ depends on the angular frequency ω. Each curve may have a low-frequency plateau, which corresponds to the DC conductivity of the material, and a dispersive region at high frequency, which corresponds to the ionic or AC conductivity. The AC conductivity, $\sigma(\omega)$; obeys the Jonscher's power law called the universal dielectric response (UDR)[40] and it is found to vary with angular frequency according to eqn(3);

$$\sigma = \sigma_{DC} + A\omega^n \quad (3)$$

where σ_{DC} is the DC conductivity, A and n are temperature-dependent parameters. Frequency dependency of conductivity at various temperatures is shown in Fig. 5.

Table 2 Activation energies and how they compare to this work.

Meas.Type	Samp.Type	Temp.Range	Act. Energy (eV)	Refs
DC	lamina Crystal	$30 > T \geq -117$	0.20 (c axis), 0.13 (ab plane)	[12]
DC	Thin film	$25 \geq T \geq -196$	0.20	[2]
DC	Bulk	$35 \geq T \geq -99$	0.175	[3]
DC	Thin film	$25 \geq T \geq -214$	0.22	[30]
DC	Bulk	$377 \geq T \geq -143$	0.26, 0.295	[10]
DC	Thin film	$127 \geq T \geq 25$	0.26	[15]
DC	Thin film	$227 \geq T \geq 25$	0.25	[34]
DC	Thin film	$742 \geq T \geq 679$	0.14	[35]
DC	Thin film	$467 > T \geq 25$	0.26, 0.23, 0.11	[36]
DC	Bulk	$711 \geq T \geq 25$	0.27 (LT), 0.08 (HT)	This study
AC	Bulk	$375 \geq T \geq 25$	0.22	This study

It can be observed that at low frequencies, the real part of conductivity, $\sigma'(\omega)$ is indeed independent of frequency giving rise to DC conductivity while at high frequencies, AC conductivity is dominant.

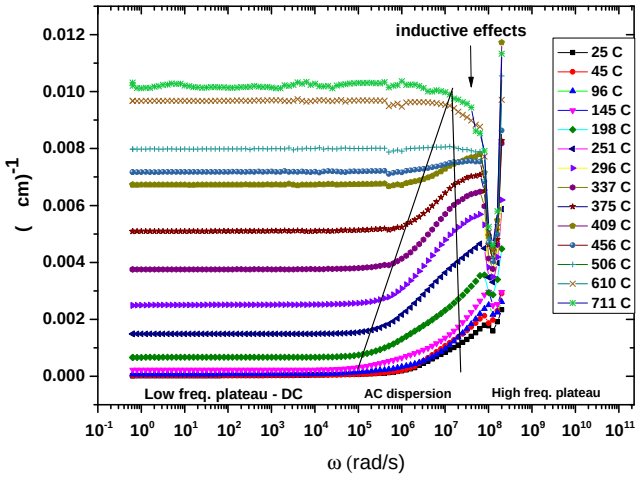

Fig. 5 Frequency dispersion of the real part of the conductivity of CAO at different temperatures.

The existence of such a dispersive regime in the conductivity at higher frequencies rules out the possibility of random hopping of mobile ions and suggests that ionic motion is somehow correlated. The crossover frequency, the frequency at which AC conductivity sets in is temperature dependent. Just as has been shown in the Fig. 4, the existence of both the DC and high frequency dispersion in Fig. 5 confirms that CAO is indeed a mixed conductor. In addition, the figure also confirms the disapperance of ionic conductivity and dominance of DC conductivity at high temperatures and sets in at $T > 375$ °C, the result also observed in Figs. 3 and 4.

At high temperatures, and at much higher frequencies, there is a second plateau also observed by other workers[41] believed to be due to excitation of Einstein oscillators and transverse optical phonons. This was observed in Na-(β/β'')-Alumina. Furthermore, at high temperature and frequency, inductive effects are also observed which may indicate ion adsorption. It may explain why copper was observed in the Pt electrode after the measurements leaving an interface rich with copper-deficient aluminate, $CuAl_2O_4$ as explained in Section 3.3.1.

Non linear curve fitting using the allometric power function in origin software was used to fit every single curve of Fig. 5 to obtain the values of n, A and σ_{DC}. The goodness of the fit were greater than 98%. The DC conductivity obtained was in perfect agreement with the actual DC measurements obtained using a two point probe, bar the slight deviation of about 10% on temperatures above 375 °C when the material is purely non ionic conducting. This is shown in Fig. 6. The deviation at high temperatures is because of contribution from DC conductivity of the material and electrode contribution because at high temperature electrode contribution dominates impedance data also[42].

The values of n in eqn(3) were found to range from 0.5-0.85, and showed no systematic temperature dependence. The value of n might have a physical meaning according to Funke[41] and Vijaykumar *et al.*[43]. For instance, value of $n < 1$ would mean that the hopping motion involved is a translational motion with a big hop[43].

This journal is © The Royal Society of Chemistry [year]

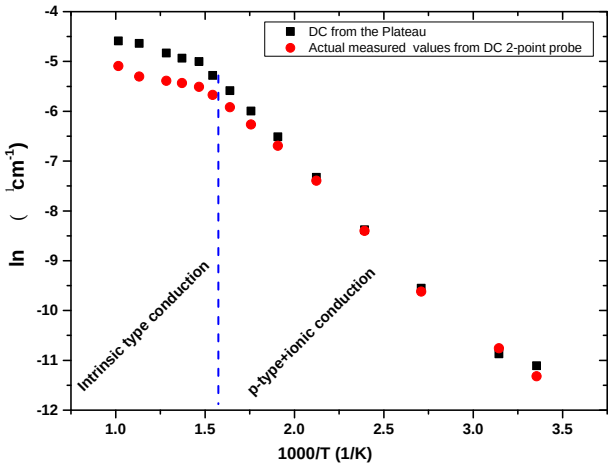

Fig. 6 An Arrhenius plot to compare the DC conductivity of the actual measured values against the low frequency values.

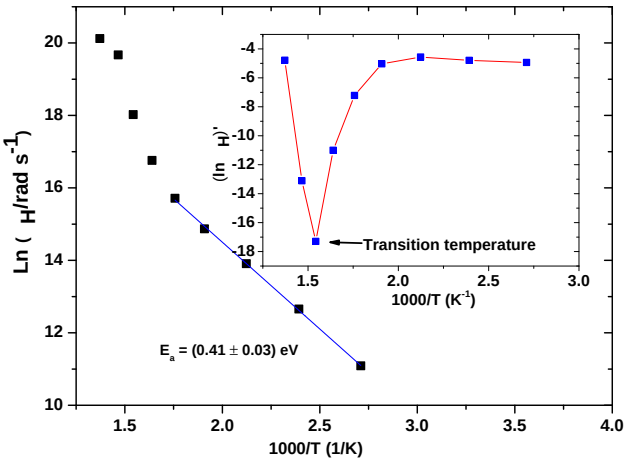

Fig. 7 Temperature dependence of hopping rate for CAO. There is a change of slope at temperatures greater than 375 °C. The inset is a first derivative of $\ln \omega_H$ denoted as $(\ln \omega_H)'$ with respect to $1000/T$. The transition point is evident.

On the other hand, value of $n \geq 1$ would mean that the motion involved is a localized hopping of the species with a small hop without leaving the neighborhood. In this case, for CAO, the transport phenomena is a long range hopping from one vacancy site to another.

To determine the hopping frequency, ω_H, the Almond and West formalism[44] was used. This is expressed as

$$\omega_H = \left(\frac{\sigma_{DC}}{A}\right)^{1/n} \tag{4}$$

with A and n being temperature dependent parameters obtained from the nonlinear function fitting of the conductivity spectra of Fig. 5 at different temperatures. The hopping frequency which is a function of temperature was then fitted to eqn(5)

$$\omega_H = \omega_o \exp(-E_\omega/kT) \tag{5}$$

where ω_o is the pre-exponential factor of the hopping rate and E_ω is hopping activation energy. The activation energy for hopping is obtained from Fig. 7 and eqn(5). The inset of Fig. 7 shows the transition temperature when the first derivative of $\ln \omega_H$ denoted as $(\ln \omega_H)'$ with respect to $1000/T$ is plotted.

The activation energy of hopping obtained ($E_\omega = 0.41$ eV) obtained was higher than the DC activation energy obtained from the Arrhenius equation ($E_a = 0.27$ eV) in eqn(1). This value is however close to the value (0.40 eV) obtained by other workers[45]. This implies that the charge carriers have to overcome less energy barrier while conducting than relaxing.

4 Conclusion

Synthesis of a phase pure delafossite $CuAlO_2$ through the conventional high temperature processing of mixed component oxides, Cu_2O and Al_2O_3 has always been obtained after prolonged reaction time some as long as 4 days. In this paper we have reported a process of pelletising component oxides followed by isothermal calcination in argon environment and quenching under graphite crucible which can be employed to reduce the reaction time down to 1.5 h. A single phase $CuAlO_2$ can be easily synthesized from mixed component oxides as long as the powder has been pelletised regardless of the amount of load applied. High temperature electrical measurements show that the material is a mixed conductor (holes and ions) up to about 375 °C beyond which the intrinsic type behavior completely dominates, the result also confirmed by the spectral analysis. Spectral analysis also revealed that conduction is of long range hopping. The LT activation energy from DC measurements was, $E_a(LT) = 0.27$ eV and high temperature value, $E_a(HT) = 0.08$ eV while the LT activation energy for ionic conductivity was $E_a(LT) = 0.22$ eV. The transition from p-type to intrinsic type conduction occurs at around 375 °C in $CuAlO_2$. We have also shown for the first time that Pt can catalyse the inadvertent formation of $CuAl_2O_4$ spinel from $CuAlO_2$, former being an insulator whereas the latter is a good p-type conductor. This is in complete agreement with the current understanding of the thermodynamic principles of Cu−Cr−O and Cu−Y−O ternary systems[46–48].

Acknowledgements

Funding from the Commonwealth Scholarship Council and the School of Chemical and Process Engineering is greatly appreciated.

References

1 L. Torkian and M. M. Amini, *Mater. Lett.*, 2009, **63**, 587–588.
2 H. Kawazoe, H. Yasakawa, H. Hyodo, M. Kurita, H. Yanagi and H. Hosono, *Nature*, 1997, **389**, 939–942.
3 Z. Deng, X. Zhu, R. Tao, W. Dong and X. Fang, *Mater. Lett.*, 2007, **61**, 686–689.
4 R. G. Gordon, *Mater. Res. Bull.*, 2000, **25**, 52–57.
5 M. Ohashi, Y. Iida and H. Morikawa, *J. Amer. Ceram. Soc.*, 2002, **85**, 270–272.
6 D. O. Scanlon and G. W. Smith, *J.Phys. Chem. Lett.*, 2010, **1**, 3195–3199.
7 D. O. Scanlon, A. Walsh and G. W. Smith, *Chem. Mater*, 2009, **21**, 4568–4576.
8 A. Kudo, A. Walsh and G. W. Watson, *Appl.Phys.Lett.*, 1998, **73**, 220–222.
9 K. Koumoto, H. Koduka and W. S. Seo, *J.Mater.Chem.*, 2001, **11**, 251–252.
10 O. J. Dura, R. Boada, A. R. Calzada, C. Leon, E. Bauer, M. A. L. de la Torre and J. Chaboy, *Phys. Rev. B*, 2011, **83**, 045202 (1–9).
11 P. A. Lee and J. B. Pendry, *Phys. Rev. B*, 1975, **11**, 2795.
12 M. S. Lee., T. Y. Kim and D. Kim, *Appl. Phys. Lett.*, 2001, **79**, 2028–2030.
13 C. Bouzidi, H. Bouzouita, A. Timoumi and B. Rezig, *Mater. Sci. Eng. B*, 2005, **118**, 259–263.
14 H. Gong, Y. Wang and Y. Luo, *Appl. Phys. Lett.*, 2000, **76**, 3959–3961.
15 A. N. Banerjee, S. Kundoo and K. K. Chattopadhyay, *Thin Solid Films*, 2003, **440**, 5–10.
16 A. N. Banerjee and K. K. Chattopadhyay, *Appl. Surf. Sci.*, 2004, **225**, 243–249.
17 C. T. Su, H. Y. Lee and M. Y. Chern, *J.Cryst. Growth*, 2011, **328**, 25–29.
18 Y. Zhang, Z. Liu, D. Zang and L. Feng, *Vacuum*, 2014, **99**, 160–165.
19 H.-C. Lu, J.-L. Lu, C.-L. Chu, C.-Y. Lai and G. mei Wu, IEEE International Nanoelectronics Conference, 2008, pp. 485–488.
20 D. Xiong, X. Zeng, W. Zhang, H. Wang, X. Zhao, W. Chen and Y.-B. Cheng, *Inorg.Chem*, 2014, **53**, 4106–4116.
21 J. Ahmed, C. K. Blakely, J. Prakash, S. R. Bruno, M. Yu, Y. Wu and V. V. Poltavets, *Journal of Alloys and Compounds*, 2014, **591**, 275–279.
22 J. Pellicer-Porres, A. Segura, C. Ferra-Roca, A. Polian, P. Munsch and D. Kim, *J. Phys.: Condens.Matter*, 2013, **25**, 115406.
23 B. J. Ingram, G. B. Gonzalez and T. O. Mason, *Chem. Mater.*, 2004, **16**, 5616–5622.
24 A. P. Amrute, Z. Lodziana, C. Mondelli, F. Krumeich and J. Perez-Ramirez, *Chem. Mater*, 2013, **25**, 4423–4435.
25 T. V. Thu, P. D. Thanh, K. Suekuni, N. H. Hai, D. Mott, M. Koyano and S. Maenosono, *Mater.Res.Bull*, 2011, **46**, 1819–1827.
26 K. Vojisavljevic, B. Malic, M. Senna, S. Drnovsek and M. Kosec, *Journal of the European Ceramic Society*, 2013, **33**, 3231–3241.
27 R. H. Jarman, J. Bafia, T. Gebreslasse, B. J. Ingram and J. D. Carter, *Mater. Res. Bull.*, 2013, **48**, 3916 – 3918.
28 T. Ishiguro, A. Kitazawa, N. Mizutani and M. Kato, *J. Solid State Chem.*, 1981, **40**, 170–174.
29 C. K. Ghosh, S. R. Popuri, T. U. Maheshi and K. K. Chattopadhyay, *J. Sol-Gel Sci.Techn*, 2009, **52**, 75–81.
30 H. Yanagi, S.-I. Inoue, K. Ueda, H. Kawazoe, H. Hosono and N. Hamada, *J.Appl. Phys.*, 2000, **88**, 4159–4163.
31 T. Prakash, *Int. Nano Lett.*, 2012, **2**, 1–3.
32 K. T. Jacob and C. B. Alcock, *J.Amer. Ceram. Soc.*, 1975, **58**, 5–6.
33 F. A. Benko and F. P. Koffyberg, *J. Phys.Chem. Solids*, 1984, **45**, 57–59.
34 A. N. Banerjee, R. Maity and K. K. Chattopadhyay, *Mater. Lett.*, 2004, **58**, 10 – 13.
35 B. J. Ingram, T. O. Mason, R. Asahi, K. T. Park and A. J. Freeman, *Phys. Rev. B*, 2001, **64**, 155114.
36 Z. Q. Yao, B. He, L. Zhang, C. Q. Zhuang, T. W. Ng, S. L. Liu, M. Vogel, A. Kumar, W. J. Zhang, C. S. Lee, S. T. Lee, and X. Jiang, *Appl.Phys. Lett.*, 2012, **100**, 0621021.
37 L. I. Berger, *Semiconductor Materials*, CRC Press, 1997.
38 H. F. Wolf, *Semiconductors*, Wiley-Interscience, 1971.
39 M. Neumann-Spallart and R. Pinto, *Thin Solid Films*, 2011, **520**, 1299 –1302.
40 A. K. Jonscher, *Nature*, 1977, **267**, 673–679.
41 K. Funke, *Prog. Solid State Chem.*, 1993, **22**, 111–195.
42 S. Basu and H. S. Maiti, *Ionics*, 2010, **16**, 111–115.
43 M. Vijaykumar, S. Selvasekarapandian, M. S. Bhuvaneswari, G. K. Hiran, G. Ramprasad, R. Subramanian and P. C. Angelo, *Physica B*, 2003, **334**, 390–397.
44 D. P. Almond, G. K. Duncan and A. R. West, *Solid State Ion.*, 1983, **8**, 159–164.
45 T. Prakash, K. P. Prasad, R. Kavitha, S. Ramasamy and B. S. Murty, *J. Appl. Phys.*, 2007, **102**, 104104.
46 K. T. Jacob, G. M. Kale and G. N. K. Iyengar, *J. Mater. Science*, 1986, **21**, 2753–2758.
47 K. T. Jacob, G. M. Kale and Y. Waseda, *Thermochimica Acta*, 1992, **208**, 341–348.
48 G. M. Kale and K. T. Jacob, *Chem. Mater*, 1989, **1**, 515–519.

This journal is © The Royal Society of Chemistry [year]